İSTANBUL UNIVERSITY CERRAHPAŞA

ORIGINAL ARTICLE
Electrica 2023; 23(2): 212-221

Investigating Permanent Magnet Synchronous Generator Wind Turbine Performance During Low Voltage Using Series and Bridge Type Fault Current Limiters

Kenneth E. Okedu[1,2]

[1]Department of Electrical and Communication Engineering, National University of Science and Technology, Muscat, Sultanate of Oman
[2]Department of Electrical and Electronic Engineering, Nisantasi University, Istanbul, Turkey

Cite this article as: K. E. Okedu, "Investigating permanent magnet synchronous generator wind turbine performance during low voltage using series and bridge type fault current limiters," *Electrica*, 23(2), 212-221, 2023.

ABSTRACT

Controlling variable speed wind turbines during transient state is challenging. The use of variable speed wind turbines based on permanent magnet synchronous generator (PMSG) is on the rise due to some of the features of the wind turbine. According to the grid code requirements, grid connected wind turbine systems should achieve active power control and provide low voltage ride through (LVRT) capability. Thus, the primary target of the wind turbine control system is to keep the turbine connected to the grid during grid disturbances or failures. In this article, the Series Dynamic Braking Resistor (SDBR), and the Bridge fault current limiter (BFCL) were used to improve the LVRT of PMSG wind turbines. The topology of the PMSG grid side voltage source converter, with the SDBR and BFCL, was modeled during steady and transient states. The performance of both schemes on the PMSG was analyzed and compared during severe balanced fault scenario. In addition, a scenario without any of the schemes was also considered. For fair comparison, the PMSG wind turbine was operating at its rated speed during the low voltage and the same conditions of operation were used for all the considered scenarios. The study was done using Power System Computer Aided Design and Electromagnetic Transient Including DC.
***Index Terms*—**Low voltage ride through, permanent magnet synchronous generator, renewable energy, wind energy, wind turbines

I. INTRODUCTION

The clean nature and cheap harvesting methods of wind energy has made it popular in the globe. The main characteristics of employing permanent magnet synchronous generators (PMSGs) in wind farms are the high power capture capabilities, wide operating speed range, and better low voltage ride through (LVRT) [1]. Based on the stipulated grid codes, wind turbines should have active power control and provide LVRT capabilities [2]. Normally, during steady condition, the machine side converter (MSC) provides maximum power point tracking (MPPT), while the grid side converter (GSC) stabilizes the DC-link voltage and regulates the reactive power injected into the grid [3]. However, during low voltage scenarios, the active power grid injection is decreased because of the drop in terminal voltage [4]. Consequently, the electrical power output transported to the grid is lower than the generated mechanical power from the wind turbine [5]. As a result of the grid fault, there is a difference between the generated power and the injected power and this is kept in the dynamic elements of the system, basically in the DC-link and the turbine rotor. Thus, the DC-link voltage and rotor of the wind generator would increase during transient state. The consequences may be the overcurrent produced will damage the fragile power converters and the generator. Therefore, decreasing the power of the generator or dissipating the excess power during grid fault would preserve the DC-link voltage below its upper limit.

In the literature, there are several studies on the possibility of modifying the MSC to help stabilize the DC-link voltage during low voltage [6]. The use of MPPT approaches of tip-speed ratio control [7], feedback power signal [8], and hill climb search [9] was already reported in the literature, considering different control strategies. Because of the nonlinear nature of wind energy, nonlinear controllers like the dq vector control [10], where the traditional PID control, fuzzy control, and adaptive schemes based on direct-current topology were used in the PMSG wind turbine. The fuzzy scheme in [11] was optimally designed to improve the MPPT of PMSG wind turbine,

Corresponding author:
Kenneth E. Okedu,

E-mail:
okedukenneth@nu.edu.om or
kenokedu@yahoo.com

Received: May 12, 2022

Revised: July 14, 2022

Accepted: August 3, 2022

Publication Date: September 29, 2022

DOI: 10.5152/electrica.2022.22066

Content of this journal is licensed under a Creative Commons Attribution-NonCommercial 4.0 International License.

considering Salp swarm optimization to minimize high-dimensional cost function multi-objective as a result of the nonlinearity of the system. The neural schemes in [12] were used for the MPPT control strategy of PMSG wind turbine to achieve maximum power and optimal estimation of wind speed. The application of nonlinear feedback schemes in [13] for the PMSG wind turbine was carried out based on Hamiltonian system, where the passivity point of view was the main consideration in the controller design. The robust control in [14] was used for the PMSG system, considering its dynamic uncertainties regarding the active and reactive power flow between the wind generator and the power grid. The back stepping schemes in [15] was used for compensating the parameter uncertainties and the same time increase the power tracking efficiency of the wind generator. The predictive control was used in [16] to regulate the frequency and generate torque compensation during disturbances because of parameter variations, wind speed, and uncertainties. A higher-order sliding mode control in the PMSG wind turbine was implemented in [17], to track the maximal power of the wind generator.

The use of fault current limiters (FCLs) hardware-based solutions in wind turbines have shown good results in fulfilling the LVRT requirements of grid codes [18]. The technology of FCLs is basically superconducting fault current limiter (SFCL) type and non-superconducting fault current limiter (NSFCL) type. There are no power loss in SFCLs, with good speed control; however, their configurations are complex [19]. The technology of the NSFCLs can solve the drawbacks of SFCLs and also provide better LVRT capability [20]. The use of insulated gate bipolar transistors (IGBTs) gave way for the NSFCLs than the others. The series dynamic braking resistors (SDBRs), and bridge fault current limiters (BFCLs) with resistive, inductive, and capacitive elements, and parallel resonance type FCL (PRFCL) show considerable improvement of the performance of variable speed wind turbines.

This article investigates the performance of PMSG-based wind turbine, considering the SDBR and the BFCL topologies during LVRT. The mathematical dynamics of the power converter for the GSC of the PMSG were modeled for the SDBR and the BFCL in the PMSG wind turbine for steady and transient states. The robustness of the controllers of the PMSG wind turbine was tested, using the threshold value of the grid voltage as the switching signal during LVRT for a balanced three-phase to ground fault in power system computer aided design and electromagnetic transient including DC (PSCAD/EMTDC) environment [21].

II. OVERVIEW OF FAULT CURRENT LIMITER TOPOLOGIES

There are several types of FCLs used in the LVRT of wind turbines [22]. These FCLs have their various benefits and drawbacks; thus, their performance would be different based on the requirements. The FCLs control strategies could be broadly classified into SFCLs, NSFCLs, and magnetic fault current limiters (MFCLs) as shown in Fig. 1 [18]. Because of their strong ability of mitigating fault currents during transient, and no power loss been incurred during their operation, FCLs are currently in use in variable speed wind farms.

The SFCL could work in hybrid with superconducting magnetic energy storage for effective energy management during and after transient states, though the SFCLs have complex structure, not cheap to implement, and liquid cryogenic system is required for changing non-superconducting mode to superconducting mode. The MFCLs configuration has basically a core that is laminated, with a permanent magnet connecting the poles. The use of permanent magnets would help in limiting the high fault currents because of the large square hysteresis loop they possess. The main shortcoming of the MFCLs is that it becomes weak over time, consequently, reducing its efficiency.

The NSFCLs are cheaper compared to the SFCLs considering the same level of dynamic stability. The employed NSFCLs have power losses because of their static components. However, SFCLs with flux coupling can reduce the power loss usually found in FCLs. But the high cost incurred would discourage their implementation. In this article, the PMSG wind turbine would be investigated during transient state using the SDBR and the BFCL topologies of the NSFCLs.

III. MODELLING OF THE PERMANENT MAGNET SYNCHRONOUS GENERATOR WIND TURBINE

Figure 2 shows the complete system for a grid-connected PMSG wind turbine having full back-to-back converter. The PMSG wind turbine system shown in Fig. 2 has no gearbox; thus, there is a direct coupling between the wind turbine and the wind generator. The output of the generator is connected to the power grid by a DC-link power converter, MSC and GSC.

For modeling the system dynamics of the PMSG wind turbine, the following differential equations apply. The mechanical power extracted

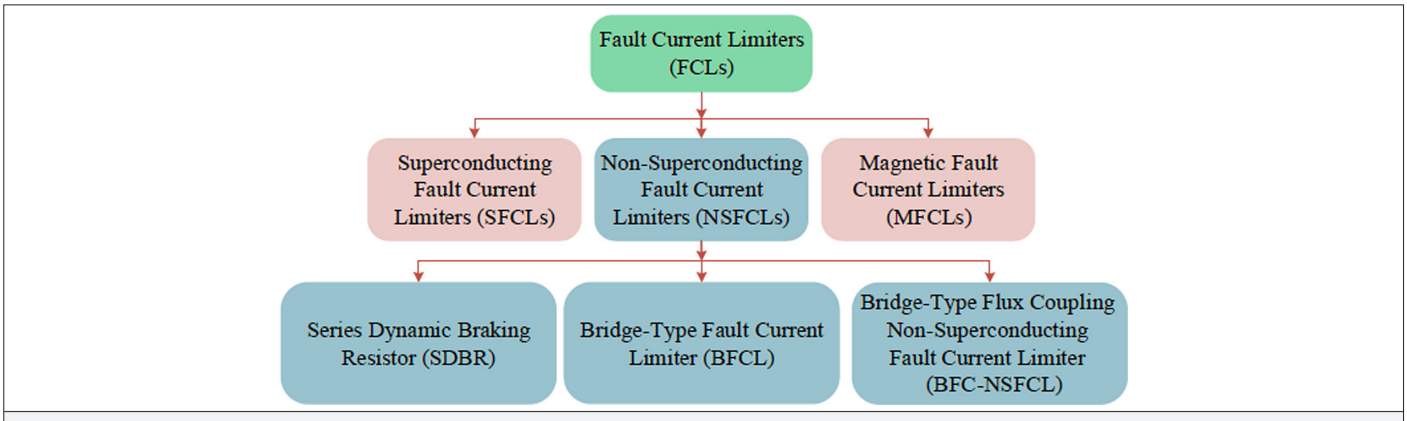

Fig. 1. Classes of fault current limiters.

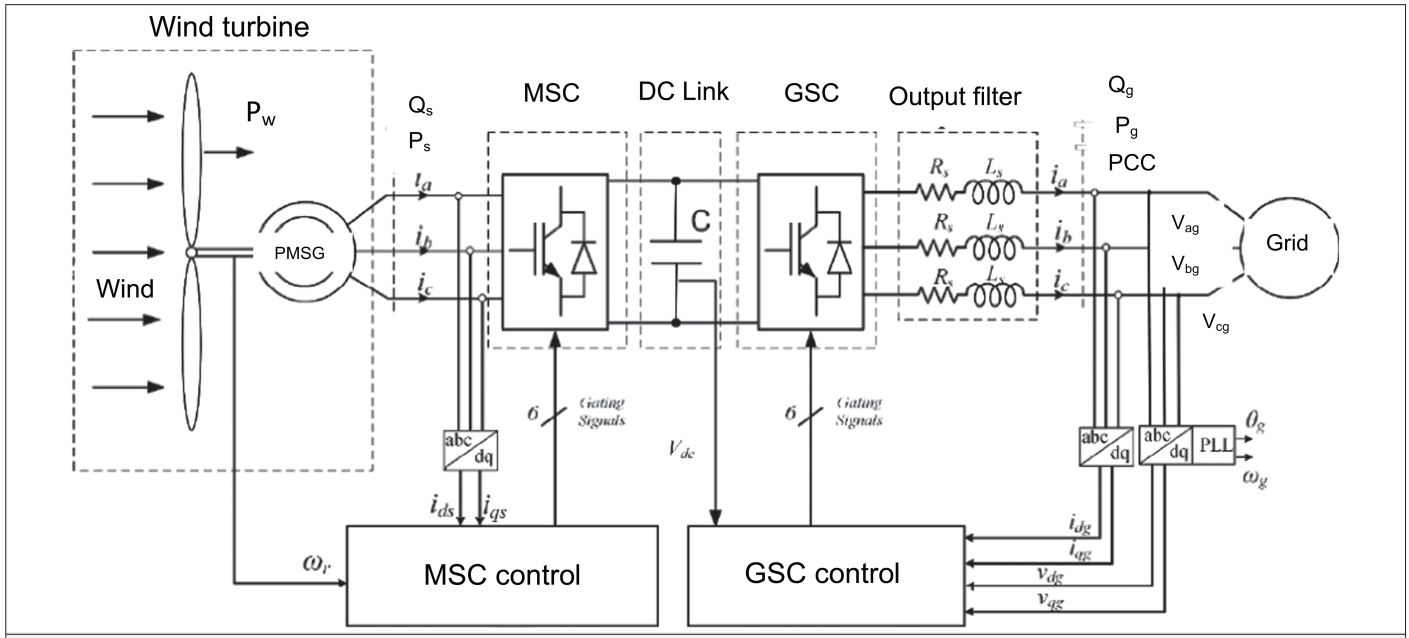

Fig. 2. PMSG wind turbine with back-to-back power converters.

(P_{wt}) and the torque (T_{wt}) of the PMSG wind turbine are expressed as [23]:

$$P_{wt} = \frac{1}{2}\rho A C_P(\lambda,\beta)V^3 \quad (1)$$

$$T_{wt} = \frac{1}{2}\frac{\rho A C_P(\lambda,\beta)V^3}{\omega_{wt}} \quad (2)$$

In (1) and (2), A is the swept area of the blade, ρ is the density of the air, C_p is the coefficient of the rotor, V is the wind speed, and ω_{wt} is the rotational speed of the wind turbine. The relationship between the tip speed ratio λ and the blade pitch angle β is given as:

$$\lambda = \frac{\omega_{wt}R}{V} \quad (3)$$

The two mass drive train model of the wind turbine mechanical system can be expressed as:

$$T_{gen} = D_m(\omega_{wt} - \omega_{gen}) + k_{sh}D_{DT} \quad (4)$$

$$\omega_{wt} = \frac{1}{2H_{\omega t}}(T_{\omega t} - T_{gen}) \quad (5)$$

where the displacement D_{DT} is given by:

$$D_{DT} = \theta_{\omega t} - \theta_{gen} \quad (6)$$

From (4)–(6), T_{gen} is the mechanical torque of the generator, D_m is the mutual damping coefficient, k_{sh} is the shaft stiffness, $H_{\omega t}$ is the per unit inertia constant, ω_{gen} is the generator's mechanical rotational speed, while $\theta_{\omega t}$ and θ_{gen} are the rotational angles of the wind turbine and the generator.

The voltage equations of the PMSG wind turbine when it operates as a grid-connected generator are given as [10]:

$$v_{ds} = -R_s i_{ds} - L_{ds}\frac{di_{ds}}{dt} + \omega_e L_{qs} i_{qs} \quad (7)$$

$$v_{qs} = -R_s i_{qs} - L_{qs}\frac{di_{qs}}{dt} - \omega_e L_{ds} i_{ds} + \omega_e \psi_f \quad (8)$$

From (7) and (8), v_{ds} and v_{qs} are the dq axes stator voltages, i_{ds} and i_{qs} are the dq axes stator currents, L_{ds} and L_{qs} are the dq axes inductances, R_s is the stator resistance, ψ_f is the rotor magnetic flux, and ω_e is the electrical angular speed given by:

$$\omega_e = p\omega_{gen} \quad (9)$$

where p is the number of pair poles. The electromagnetic torque T_e is expressed as:

$$T_e = p(\psi_f i_{qs} + (L_{ds} - L_{qs})i_{ds}i_{qs}) \quad (10)$$

The mechanical equation for the PMSG is:

$$T_{gen} - T_e = J\frac{d\omega_{gen}}{dt} \quad (11)$$

In (11), J is the total mechanical system moment of inertia. The DC-link voltage of the PMSG is affected by the extracted power flow of the generator and the injected power flow of the grid. Neglecting the power loss of the generator and the converter loss, the dynamics of the DC-link voltage V_{dc} is given as:

$$CV_{dc}\frac{dV_c}{dt} = P_{gen} - P_{grid} = T_e\omega_{gen} - P_{grid} \quad (12)$$

The PMSG wind turbine characteristics is shown in Fig. 3, for the turbine output power with different speeds, where the reference power P_{ref} is based on the rated power. The maximum power output of 1.0 pu was obtained at 12 m/s and 1.0 pu rotational speed.

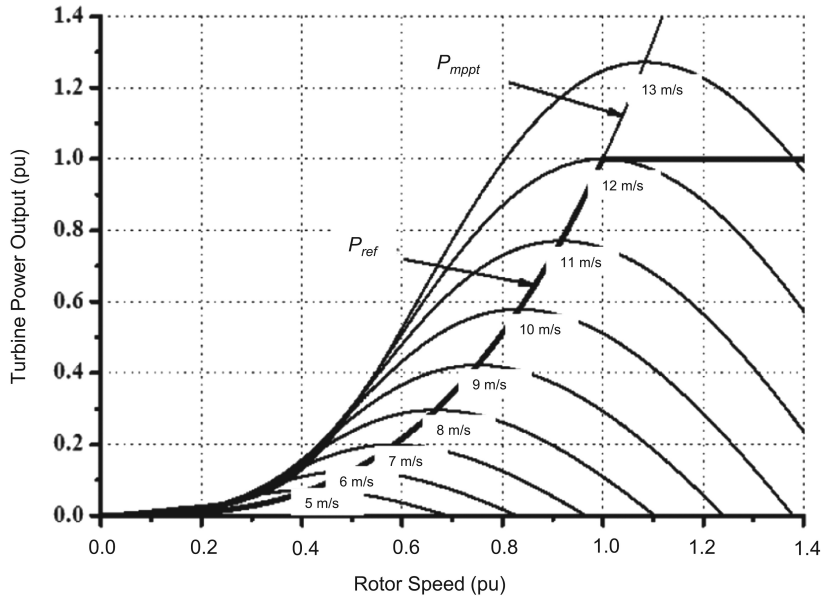

Fig. 3. The maximum power characteristics of the PMSG wind turbine.

IV. THE POWER CONVERTERS CONTROL OF THE PERMANENT MAGNET SYNCHRONOUS GENERATOR WIND TURBINE

Figure 4 shows the power converter control for the MSC and the GSC of the PMSG wind turbine. In normal condition, the MSC regulates the active power control to extract maximum wind power. The MSC of the PMSG wind turbine is shown in Fig. 4, where the rotor speed is regulated based on its reference value obtained from the MPPT characteristics in Fig. 3. In Fig. 4, the q-axis current (i_{qsref}) is generated from the proportional integral (PI) controller and the component in the d-axis (i_{dsref}) that is set to zero value. This control topology would help to achieve the required reference values, so that maximum power could be extracted and delivered to the DC-link of the PMSG wind turbine.

On the other hand, the control strategy for the GSC is shown in Fig. 5, where after obtaining the MPPT from the MSC, the reference d-axis grid current (i_{dgref}) is generated by the DC-link voltage controllers, in order to adjust the terminal voltage to its steady state value. The active and reactive power which are the injected grid power components are controlled independently. The control of the dq components is done through the PI controllers' loop that is cascaded in nature.

V. THE PERMANENT MAGNET SYNCHRONOUS GENERATOR MODEL SYSTEM WITH SERIES DYNAMIC BRAKING RESISTOR AND BRIDGE FAULT CURRENT LIMITER

The model system of this study is shown in Fig. 6. A system base of 5.0 MVA, and short circuit of 16.67 MVA, was used in the study and the PMSG wind turbine is connected to an infinite bus. The parameters of the model system are given in Table I [24, 25]. On the double circuit of the model system in Fig. 6, a severe three-phase to ground fault occurred. The SDBR and BFCL are connected to the GSC of the PMSG wind turbine. The connection of either the SDBR or BFCL to the PMSG wind turbine GSC would improve its performance during grid fault. The parameters of the SDBR and BFCL used in this study are given in Table II. The switching of the SDBR and BFCL is based on the grid voltage, during steady state (above 0.9 pu) or grid disturbance (below 0.9 pu). The mathematical dynamics of the SDBR and BFCL in the PMSG wind turbine are as follows.

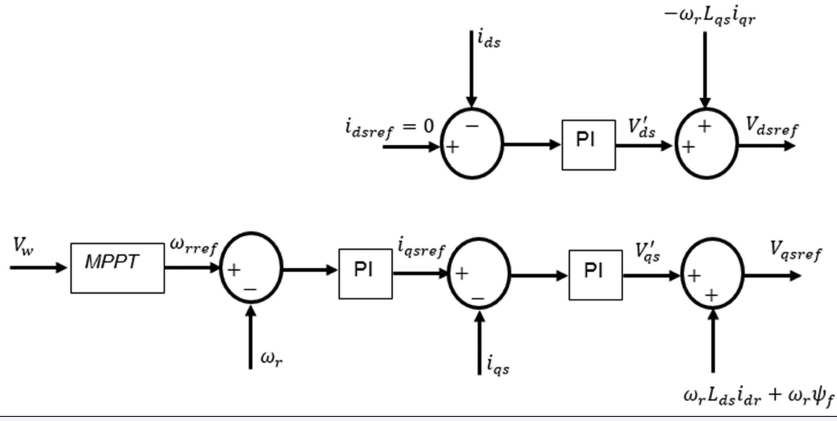

Fig. 4. The PMSG wind turbine machine side converter.

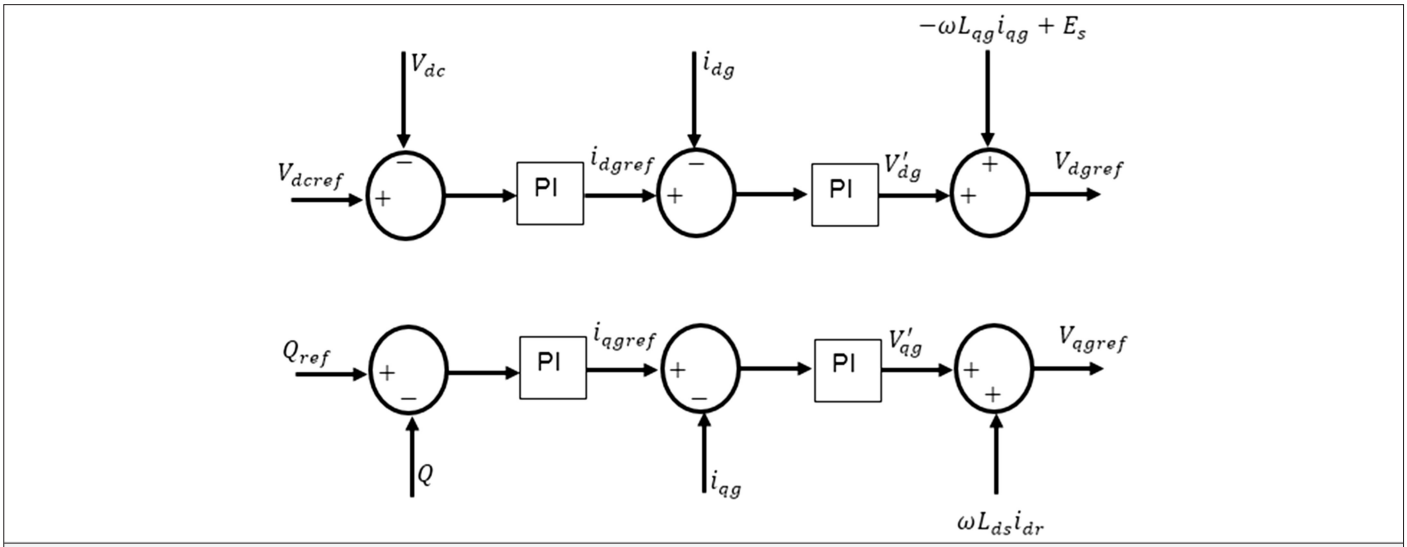

Fig. 5. The PMSG wind turbine grid side converter.

The connection of the SDBR and BFCL in the PMSG-based wind turbine as shown in Fig. 6 is based on current control topology and not voltage [26, 27]. The resistor is usually bypassed during nominal operation when the switch is conducting, based on the threshold value (0.9 pu) of the grid voltage used for switching purposes. However, during fault scenario, the switch is off. The SDBR and BFCL would limit the high rotor inrush current while operating, thus excessive active power would be achieved [28, 29]. The MSC and GSC power converters would be effectively balanced, mitigating the current in the stator and the DC-link capacitor charging, as a result of the accumulation of these effects on the PMSG wind turbine.

The control structures of the SDBR and the BFCL are shown in Fig. 6 model system. The BFCL is made up of two parts, a typical bridge

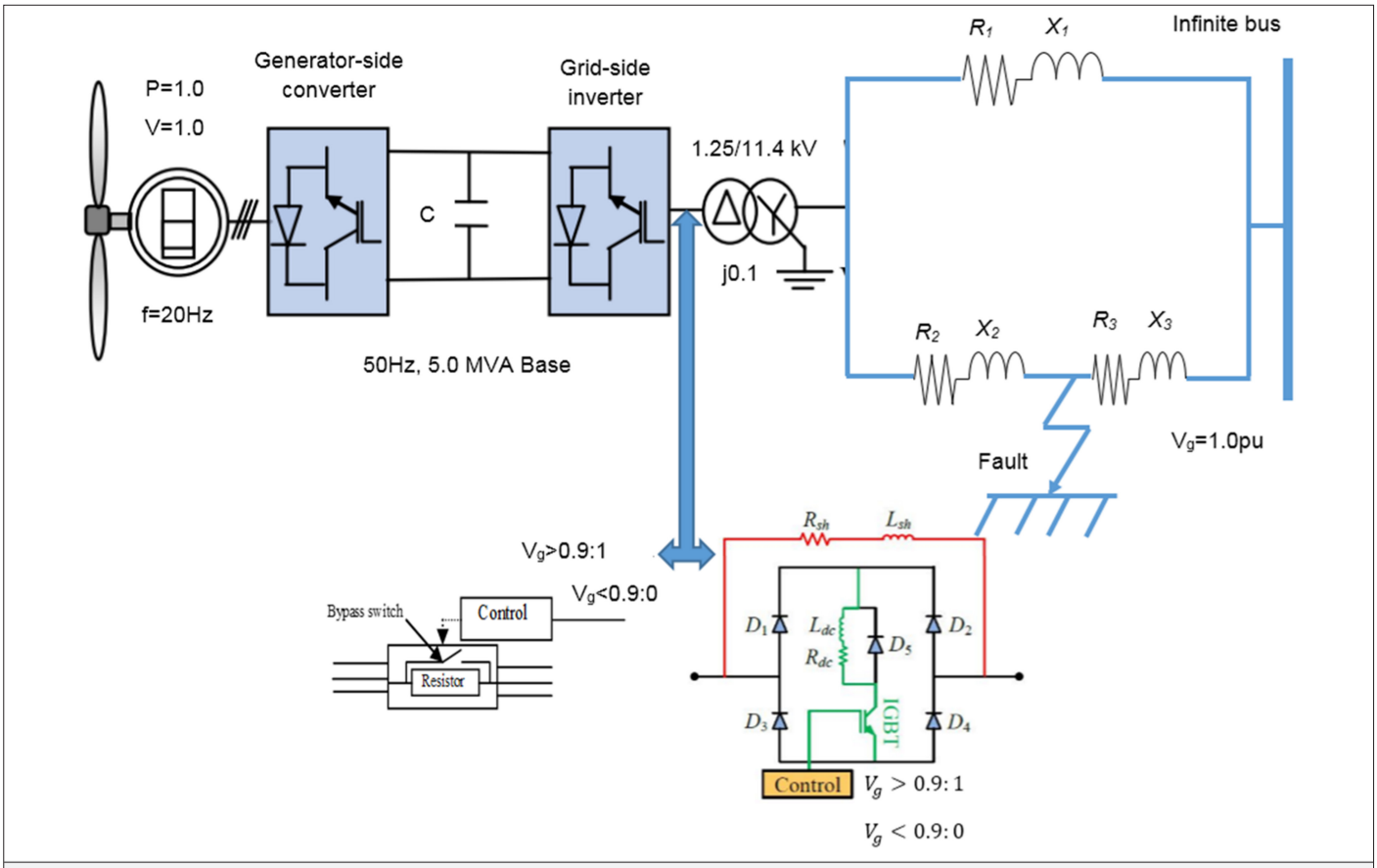

Fig. 6. Model system of PMSG wind turbine with SDBR and BFCL.

TABLE I. PARAMETERS OF THE MODEL SYSTEM

Rated power	**5.0 MW**	**Rated voltage**	**1.0 kV**
Rated voltage	1.0 kV	Field flux	1.4 pu
Frequency	20.0 Hz	Blade radius	40.0 m
Number of poles	150.0	Rated wind speed	12.0 m/s
Machine inertia	3.0	R_1	0.87120 Ω
Stator resistance	0.01 pu	R_2	0.04356 Ω
d-axis reactance	1.0 pu	R_3	0.82764 Ω
q-axis reactance	0.7 pu	X_1	5.2157 Ω
X_2	0.2608 Ω	X_3	4.9549 Ω

TABLE II. PARAMETERS OF THE FAULT CURRENT LIMITERS

SDBR	**BFCL**			
	R_{sh}	L_{sh}	R_{dc}	L_{dc}
Series resistance (R_s) 0.1 pu	20 Ω	250 mH	0.003 Ω	1 mH

SDBR, series dynamic braking resistor; BFCL, bridge fault current limiter.

circuit with four diodes (D_1–D_4) and a shunt path made up of inductor (L_{sh}) and resistor (R_{sh}) in series. There is an IGBT switch connected in series with an inductor (L_{dc}), and (R_{dc}) act as an intrinsic resistance of (L_{dc}) with very small magnitude that is negligible. In the BFCL, the (L_{dc}) inductor is a DC reactor due to the fact that current flows in one direction only during its positive and negative half cycle of the alternating current. There is a free-wheeling diode D_5 that is connected to the DC reactor to protect the system from inductive kick during transient state [30]. The principle of the BFCL during operation is such that at steady state, the current flows through the D_1-L_{dc}-R_{dc}-IGBT-D_4 path for the positive half cycle and through the D_3-IGBT-R_{dc}-L_{dc}-D_2 path for the negative half cycle. The shunt path of the BFCL has a very high impedance, thus, the line current and some negligible leakage currents are on the bridge switch [18].

The topology of the voltage source converter in wind energy conversion results in high DC-link voltage quality, capability of bidirectional flow of power, unity power factor, and low current distortions. Since the PMSG-based wind turbine is decoupled fully from the power grid as a result of its back-to-back power converter, inserting the SDBR and BFCL with the grid-connected inverter in Fig. 7 would help understand the dynamics of the SDBR and BFCL in the PMSG wind turbine GSC.

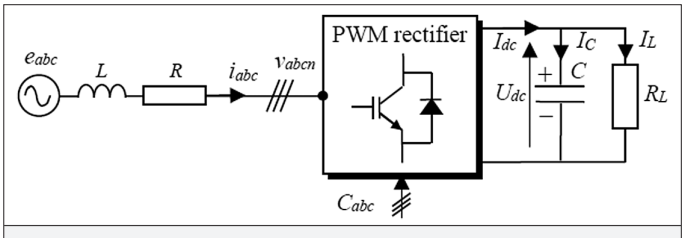

Fig. 7. Topologies of SDBR and BFCL in PMSG grid side voltage source converter.

From Fig. 7, the GSC of the PMSG wind turbine is connected to the R and L parameters of the grid, with AC currents $i = a,b,c$. If C_{abc} represents the three switching states for the IGBTs, then the C_{abc} converter functions can be substituted by β_{abc} signals of modulation. Considering Park's transformation, the voltage source converter of the PMSG could be modeled for a balanced three-phase as [18]:

$$e_d = -\omega L i_q + L\frac{di_d}{dt} + (R + R_{SDBR} \text{ or } Z_{BFCL})i_d + 0.5U_{dc}\beta_d \tag{13}$$

$$e_q = -\omega L i_d + L\frac{di_q}{dt} + \left(R + R_{SDBR} \text{ or } Z_{BFCL}\right)i_q + 0.5U_{dc}\beta_q \tag{14}$$

$$C\frac{dU_{dc}}{dt} = 0.75\left(i_d\beta_d + i_q\beta_q\right) - \frac{U_{dc}}{R_L} \tag{15}$$

$$r = \sqrt{\beta_d^2 + \beta_q^2} \tag{16}$$

From (13)–(16), i_d, i_q are dq current input of the rectifier's axes, e_d,e_q are dq voltage of the grid voltage axes components, ω is the angular frequency voltage, β_d, β_q are the rectifier's d and q axes components, while r is the modulation signal vector norm, U_{dc}, is the DC-link voltage, R_{SDBR}, is the effective SDBR resistance, Z_{BFCL} is the effective BFCL reactance, and ω is the angular frequency. The Park's principle for three-phase transformation, for phase-A grid voltage with the dq reference is:

$$e_d = E_m \tag{17}$$

$$e_q = 0 \tag{18}$$

E_m is the voltage amplitude, e_d and e_q, the d and q source voltages. The active (P_s) and reactive (Q_s) rectifier's powers are:

$$P_s = \frac{3}{2}E_m i_d \tag{19}$$

$$Q_s = -\frac{3}{2}E_m i_q \tag{20}$$

In order to obtain power factor of 1, i_{q_ref} should be 0. Therefore, for the current regulation to be ideal, $i_q = i_{qref} = 0$. Considering $i_q = 0$ and $e_q = 0$, the voltage amplitude for power factor 1 is:

$$E_m = L\frac{di_d}{dt} + (R + R_{SDBR} \text{ or } Z_{BFCL})i_d + 0.5U_{dc}\beta_d \tag{21}$$

$$\beta_q = -\frac{2\omega L}{U_{dc}}i_q \tag{22}$$

$$C\frac{dU_{dc}}{dt} = \frac{3}{4}i_d\beta_d - \frac{U_{dc}}{R_L} \tag{23}$$

For power factor of 1, the voltage source converter β_q should vary with i_q current. Thus, the capacitor charge is manipulated by β_d, via the i_d current of the input based on (21) and (23). When the SDBR and BFCL are inserted, (21)– (23) would be zero, making:

$$E_m = (R + R_{SDBR} \text{ or } Z_{BFCL})i_d + 0.5U_{dc}\beta_d \tag{24}$$

$$\beta_q = -\frac{2\omega L}{U_{dc}}i_q \tag{25}$$

$$i_d = \frac{4U_{dc}}{3\beta_d R_L} \tag{26}$$

For a load R_L and voltage U_{dc}, β_d is

$$6E_m R_L \beta_d - 8\left(R + R_{SDBR} \text{ or } Z_{BFCL}\right)U_{dc} - 3R_L\beta_d^2 U_{dc} = 0, for\ \beta_d \neq 0 \tag{27}$$

Giving two solutions:

$$\beta_{d1} = \frac{E_m}{U_{dc}} - \sqrt{\left(\frac{E_m}{U_{dc}}\right)^2 - \frac{8\left(R + R_{SDBR} \text{ or } Z_{BFCL}\right)}{3R_L}} \tag{28}$$

$$\beta_{d2} = \frac{E_m}{U_{dc}} + \sqrt{\left(\frac{E_m}{U_{dc}}\right)^2 - \frac{8\left(R + R_{SDBR} \text{ or } Z_{BFCL}\right)}{3R_L}} \tag{29}$$

Solution of β_d in (28) is not feasible because it has very low values. However, solution of (29) is acceptable making $\beta_d = \beta_{d2}$ and β_d would exist if:

$$\left(\frac{E_m}{U_{dc}}\right)^2 - \frac{8\left(R + R_{SDBR} \text{ or } Z_{BFCL}\right)}{3R_L} \geq 0 \tag{30}$$

But

$$P_{dc} \leq P_{dc\_max} \tag{31}$$

where P_{dc_max} is the PMSG converter maximum, and from power conservation principle, P_{dc_max} could be expressed as:

$$P_{dc} = \frac{3}{2}E_m i_d - \frac{3}{2}\left(R + R_{SDBR} \text{ or } Z_{BFCL}\right)i_d^2 \tag{32}$$

If $dP_{dc}/di_d = 0$, the maximum power transfer to the DC would be:

$$\frac{dP_{dc}}{di_d} = \frac{3}{2}E_m - 3Ri_d = 0 \rightarrow i_d = i_{d\_max} = \frac{E_m}{2R} \tag{33}$$

Substituting (33) into (32):

$$P_{dc\_max} = \frac{3E_m^2}{8\left(R + R_{SDBR} \text{ or } Z_{BFCL}\right)} \tag{34}$$

and the voltage source converter operation is possible when

$$P_{dc} \leq P_{dc\_max} \rightarrow \left(\frac{E_m}{U_{dc}}\right)^2 - \frac{8\left(R + R_{SDBR} \text{ or } Z_{BFCL}\right)}{3R_L} \geq 0 \tag{35}.$$

The grid input maximal power P_{s_max} can be obtained by putting (34) into (20) for Q_s. Thus:

$$P_{s\_max} = \frac{3E_m^2}{4\left(R + R_{SDBR} \text{ or } Z_{BFCL}\right)} \tag{36}$$

Therefore, during transient state, the maximum power transfer in the GSC of the PMSG, and the total current would be reduced. The oscillations that usually occur would also be less because of the control strategies of the SDBR and the BFCL.

VI. EVALUATION OF THE SYSTEM PERFORMANCE

The model system of the PMSG wind turbine with the SDBR and BFCL was carried out in PSCAD/EMTDC environment. The model system was subjected to a severe symmetrical three-phase fault of 100 ms happening at 10.1 s, with the circuit breakers operation sequence opening and reclosing at 10.2 s and 11 s respectively. The model system was evaluated considering three scenarios. In the first scenario, no control strategy of FCL was employed in the PMSG wind turbine. In the second scenario, the SDBR FCL control strategy was used in the PMSG wind turbine, while the BFCL was implemented in the third scenario. The PMSG wind turbine was operating at its rated speed during the grid fault. Some of the PMSG wind turbine variables are shown in Figs 8–12, for the three scenarios considered in this study.

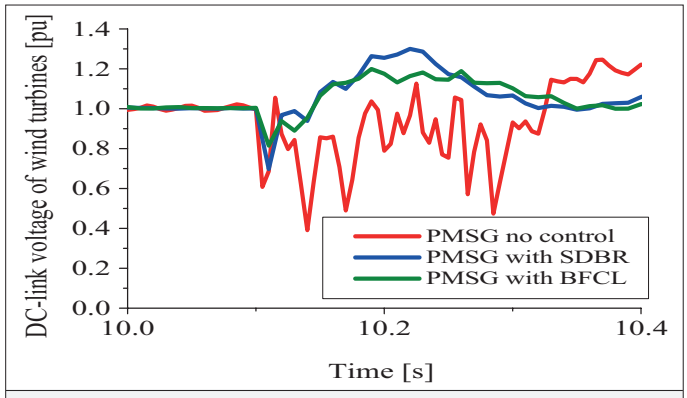

Fig. 8. DC-link voltage of the PMSG wind turbine for all scenarios

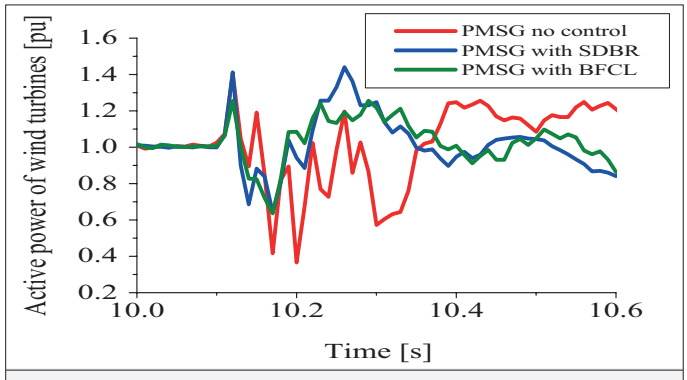

Fig. 9. Active power of the PMSG wind turbine for all scenarios.

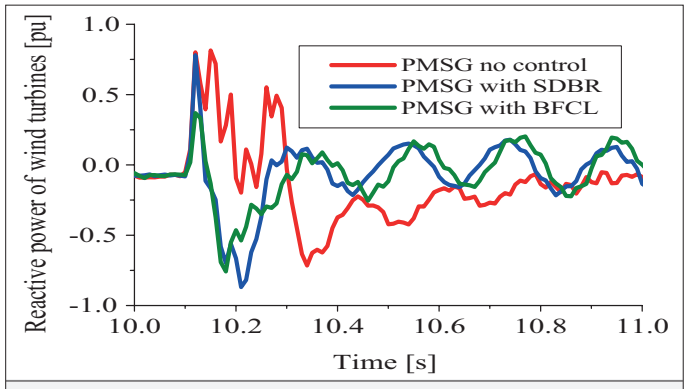

Fig. 10. Reactive power of the PMSG wind turbine for all scenarios.

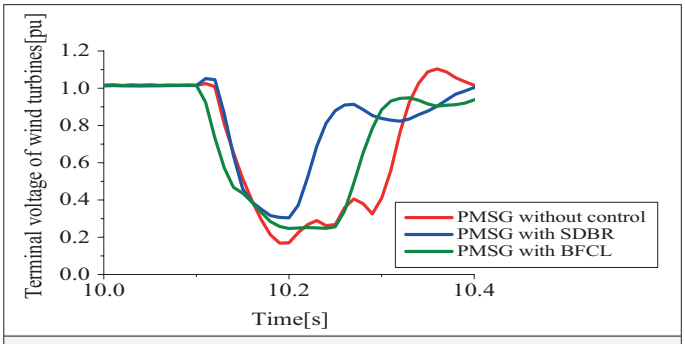

Fig. 11. Terminal voltage of the PMSG wind turbine for all scenarios.

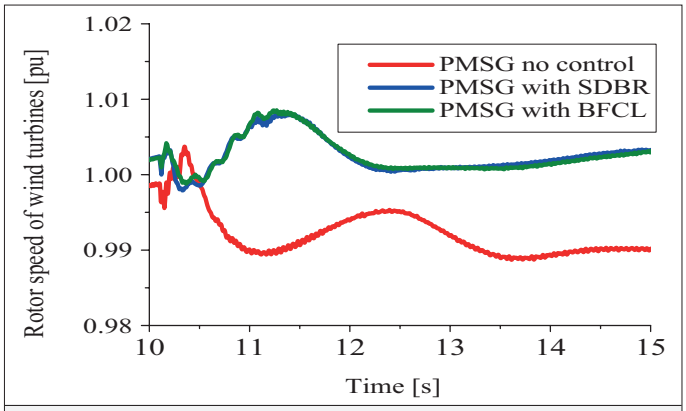

Fig. 12. Rotor speed of the PMSG wind turbine for all scenarios.

Figures 8 and 9 show the DC-link voltage and active power of the PMSG wind turbine for no control strategy, using FCL with SDBR, and with BFCL control strategies. It is obvious from Figs. 8 and 9 that connecting SDBR and BFCL on the PMSG wind turbine GSC would improve the DC-link voltage and active power variables during grid fault because of the decoupling of the PMSG wind turbine by the grid based on its back-to-back power converter. Using the metrics of the overshoot, undershoot and settling time of the variables of the wind generator, scenarios where the SDBR and BFCL were implemented, gave better responses than no control scenario. One of the technical reasons for this is based on the fact that connecting the SDBR and BFCL on GSC of the PMSG, divides the expected high voltage in the stator circuitry of the PMSG wind turbine, since it is a series connection topology, based on the mathematical dynamics of their connection earlier explained. The performance of the BFCL is better than SDBR because of the additional energy buffer from the inductive circuit of the BFCL.

Figure 10 shows that the reactive power was better controlled and dissipated during transient state using the BFCL than the SDBR and no control scenarios. This is because the inductive circuit would act as an energy buffer to the PMSG wind turbine, thereby controlling its reactive power. Consequently, the terminal voltage of the PMSG wind turbine would be improved as shown in Fig. 11, since reactive power is directly proportional to voltage. The voltage variable of the PMSG wind turbine settled faster using the BFCL than the SDBR and no control scenarios. Though the SDBR gave low voltage dip and the same overshoot as the BFCL, however, its settling time is more than that of the BFCL control strategy.

In Fig. 12, the performance of the rotor speed of the PMSG wind turbine is better with the use of SDBR and BFCL than the scenario without control. The rotor speed responses for the SDBR and BFCL scenarios are the same because their control techniques in the PMSG wind turbine has the capability to enhance the mechanical output, and the same time limit the speed during grid disturbances. These effects would lead to fewer oscillations, and improved settling time. Based on the presented results, employing the SDBR and BFCL at the GSC of the PMSG wind turbine give room for no induced overvoltage, no loss of power converter control, mitigation of high current flow, and no excessive charging current in the capacitor of the DC-link voltage of the wind generator.

VII. CONCLUSION

In this article, the performance of the PMSG wind turbine was investigated using SDBR and BFCL. The grid voltage set value during grid fault was used as the switching signal for the IGBTs of both FCLs, for fair comparison. A severe symmetrical three-phase to ground fault at the terminals of the PMSG was applied to test the robustness of both protection schemes. Three scenarios were investigated for the PMSG wind turbine; no control strategy, with SDBR at the GSC, and with BFCL at the GSC. When no control was implemented, there were substantial effects on the PMSG during transient state. Apparently, using the SDBR and BFCL would enhance the PMSG wind turbine performance. The performance of the BFCL was superior to that of the SDBR during transient state. Therefore, the BFCL would help solve fault ride through capability of PMSG wind farms even though its structure is complex, more than the simple SDBR topology.

Peer-review: Externally peer-reviewed.

Declaration of Interests: The author has no conflicts of interest to declare.

Funding: The author declared that this study has received no financial support.

REFERENCES

1. H. M. Yassin, H. H. Hanafy, and M. M. Hallouda, "Enhancement Low voltage ride through capability of permanent magnet synchronous generator-based wind turbines using interval type-2 fuzzy control," *IET Renew. Power Gener.*, vol. 10, no. 3, pp. 339–348, 2016. [CrossRef]
2. M. Tsili, and S. Papathanassiou, "A review of grid code technical requirements for wind farms," *IET Renew. Power Gener.*, vol. 3, no. 3, pp. 308–332, 2009. [CrossRef]
3. J. Chen, W. Yao, C. K. Zhang, Y. Ren, and L. Jiang, "Design of robust MPPT controller for grid-connected PMSG-Based wind turbine via perturbation observation based nonlinear adaptive control," *Renew. Energy*, vol. 134, pp. 478–495, 2019. [CrossRef]
4. J. F. Conroy, and R. Watson, "Aggregate modelling of wind farms containing full-converter wind turbine generators with permanent magnet synchronous machines: Transient stability studies," *IET Renew. Power Gener.*, vol. 3, no. 1, pp. 39–52, 2009. [CrossRef]
5. S. Alepuz, S. Busquets-Monge, J. Bordonau *et al.*, "Control strategies based on symmetrical components for grid-connected converters under voltage dips," *IEEE Trans. Ind. Electron.*, vol. 56, no. 6, pp. 2162–2173, 2009. [CrossRef]
6. S. Alepuz, A. Calle, S. Busquets-Monge, S. Kouro, and B. Wu, "Use of Stored Energy in PMSG Rotor Inertia for Low-Voltage Ride-Through in Back-to-Back NPC Converter-Based Wind Power Systems" *IEEE Trans. Ind. Electron.*, vol. 60, no. 5, pp. 1787–1796, 2013. [CrossRef]
7. P. Chen, D. Han, and K.-C. Li, "Robust adaptive control of maximum Power Point tracking for wind power system," *IEEE Access*, vol. 8, pp. 214538–214550, 2020. [CrossRef]

8. S. M. Barakati, M. Kazerani, and J. D. Aplevich, "Maximum power tracking control for a wind turbine system including a matrix converter," *IEEE Trans. Energy Convers.*, vol. 24, no. 3, pp. 705–713, 2009. [CrossRef]
9. M. Karabacak, L. M. Fernandez-Ramirez, T. Kamal, and S. Kamal, "A New Hill climbing maximum power tracking control for wind turbines with inertial effect compensation," *IEEE Trans. Ind. Electron.*, vol. 66, no. 11, pp. 8545–8556, 2019. [CrossRef]
10. S. Li, T. A. Haskew, and L. Xu, "Conventional and novel control designs for direct driven PMSG wind turbines," *Electr. Power Syst. Res.*, vol. 80, no. 3, pp. 328–338, 2010. [CrossRef]
11. M. Qais, H. M. Hasanien, and S. Alghuwainem, "Salp swarm algorithm-based TS-FLCs for MPPT and fault ride-through capability enhancement of wind generators," *ISA Trans.*, vol. 101, pp. 211–224, 2020. [CrossRef]
12. R. Sitharthan, M. Karthikeyan, D. S. Sundar, and S. Rajasekaran, "Adaptive hybrid intelligent MPPT controller to approximate effectual wind speed and optimal rotor speed of variable speed wind turbine," *ISA Trans.*, vol. 96, pp. 479–489, 2020. [CrossRef]
13. Y. Gui, C. Kim, and C. C. Chung, "Improved low-voltage ride through capability for PMSG wind turbine based on port-controlled Hamiltonian system," *Int. J. Control Autom. Syst.*, vol. 14, no. 5, pp. 1195–1204, 2016. [CrossRef]
14. S. Das, and B. Subudhi. A H∞ robust active and reactive power control scheme for a PMSG-based wind energy conversion system," *IEEE Transactions on Energy Conversion*, vol. 33, no. 3, pp. 980–990, 2018.
15. M. Ayadi, and N. Derbel, "Nonlinear adaptive backstepping control for variable-speed wind energy conversion system-based permanent magnet synchronous generator," *Int. J. Adv. Manuf. Technol.*, vol. 92, no. 1–4, pp. 39–46, 2017. [CrossRef]
16. H. X. Wang *et al.* "Model predictive control of PMSG-based wind turbines for frequency regulation in an isolated grid," *IEEE Trans. Ind. Appl.*, vol. 54, no. 4, pp. 3077–3089, 2018. [CrossRef]
17. B. Yang *et al.*, "Passivity-based sliding-mode control design for optimal power extraction of a PMSG based variable speed wind turbine," *Renew. Energy*, vol. 119, pp. 577–589, 2018. [CrossRef]
18. M. R. Islam et al., "Fault ride through capability improvement of dfig based wind farm using nonlinear controller based bridge-type flux coupling non-superconducting fault current limiter," *Energies*, vol. 13, no. 7, p. 1696, 2020. [CrossRef]
19. M. Firouzi, "Low-voltage ride-through (lvrt) capability enhancement of dfig-based wind farm by using bridge-type superconducting fault current limiter (btsfcl)," *J. Power Technol.*, vol. 99, no. 4, pp. 245–253, 2020.
20. G. Rashid, and M. H. Ali, "A modified bridge-type fault current limiter for fault ride-through capacity enhancement of fixed speed wind generator," *IEEE Trans. Energy Convers.*, vol. 29, no. 2, pp. 527–534, 2014. [CrossRef]
21. PSCAD/EMTDC User's Guide Manual; Version 4.6.0; Manitoba HVDC Lab.: Winnipeg, MB, Canada, 2016.
22. H. Radmanesh, S. H. Fathi, G. B. Gharehpetian, and A. Heidary, "Bridge-type solid-state fault current limiter based on AC/DC reactor," *IEEE Trans. Power Deliv.*, vol. 31, no. 1, pp. 200–209, 2015. [CrossRef]
23. I. Sami, S. Ullah, N. Ullah, and J. S. Ro, "Sensorless fractional order composite sliding mode control design for wind generation system," *ISA Trans.*, vol. 111, pp. 275–289, 2021. [CrossRef]
24. K. E. Okedu, and H. Barghash, "Enhancing the transient state performance of permanent magnet synchronous generator based variable speed wind turbines using power converters excitation parameters," *Front. Energy Res.*, vol. 9, pp. 109–120, Article 655051, April, 2021. [CrossRef]
25. K. E. Okedu, and S. M. Muyeen, "Enhanced performance of PMSG Wind Turbines during grid disturbance at different network strengths considering fault current limiter," *Int. Trans. Electr. Energy Syst. Wiley*, vols. 1–21, no. June, p. e12985, 2021. [CrossRef]
26. K. E. Okedu, S. M. Muyeen, R. Takahashi, and J. Tamura, "Wind farms fault ride through using DFIG with new protection scheme," *IEEE Trans. Sustain. Energy*, vol. 3, no. 2, pp. 242–254, 2012. [CrossRef]
27. K. E. Okedu, "Effect of ECS low pass filter timing on grid frequency dynamics of a power network considering wind energy penetration," *IET Renew. Power Gener.*, vol. 11, no. 9, pp. 1194–1199, 2017. [CrossRef]
28. K. E. Okedu, "Determination of the most effective switching signal and position of braking resistor in DFIG wind turbine under transient conditions," *Electr. Eng.*, vol. 102, no. 1, pp.471–480, 2020. [CrossRef]
29. K. E. Okedu, S. M. Muyeen, R. Takahashi, and J. Tamura, "Wind farm stabilization by using DFIG with current controlled voltage source converters taking grid codes into consideration," *IEEJ Trans. Power Energy*, vol. 132, no. 3, pp. 251–259, 2012. [CrossRef]
30. K. E. Okedu, S. M. Muyeen, R. Takahashi, and J. Tamura, "Improvement of fault ride through capability of wind farm using DFIG considering SDBR", 14th Eur. Conference of Power Electronics EPE. Birmingham, United Kingdom, 2011, pp. 1–10.

Kenneth Eloghene Okedu was a research fellow in the Department of Electrical and Computer Engineering, Massachusetts Institute of Technology (MIT), Boston, USA, in 2013. He obtained his Ph.D. from the Department of Electrical and Electronic Engineering, Kitami Institute of Technology, Japan, in 2012. He received his BSc and MEng in Electrical and Electronic Engineering from the University of Port Harcourt, Nigeria, in 2003 and 2007, respectively, where he was retained as a faulty member from 2005 until the present day. He has also been a visiting faculty member at the Abu Dhabi National Oil Company (ADNOC) Petroleum Institute. He was also a visiting faculty member at the Caledonian College of Engineering, Oman (Glasgow Caledonian University, UK). He is presently a visiting professor in the Department of Electrical and Computer Engineering, National University of Science and Technology (NUST), Oman, and an adjunct professor in the Department of Electrical and Electronic Engineering, Nisantasi University, Turkey. He was recognized as a top 1% peer reviewer in Engineering by Publons in 2018 and 2019 and was the editor's pick in the *Journal of Renewable and Sustainable Energy* in 2018. Dr. Okedu has published several books and journals/transactions in the field of renewable energy. He is an editor for including Frontiers in Renewable Energy Research (Smart Grids), Energies (MDPI), *International Journal of Smart Grids*, *International Journal of Electrical Engineering*, *Mathematical Problems in Engineering*, and *Trends in Renewable Energy*. His research interests include power system stability, renewable energy systems, stabilization of wind farms, stability analysis of doubly-fed induction generators (DFIGs) and permanent magnet synchronous generators (PMSG), variable speed wind turbines, augmentation and integration of renewable energy into power systems, grid frequency dynamics, wind energy penetration, FACTS devices and power electronics, renewable energy storage systems, and hydrogen and fuel cells.